

Spin fluctuations in $Y(\text{Co}_{1-x}\text{Al}_x)_2$: A transition system from nearly to weakly itinerant ferromagnetism

K. Yoshimura and M. Mekata

Department of Applied Physics, Fukui University, Bunkyo, Fukui 910, Japan

M. Takigawa,* Y. Takahashi, and H. Yasuoka

Institute for Solid State Physics, University of Tokyo, Roppongi, Minato-ku, Tokyo 106, Japan

(Received 29 June 1987)

The magnetic susceptibility χ , the Knight shift K , and the nuclear spin-lattice relaxation rate $1/T_1$ have been measured in $Y(\text{Co}_{1-x}\text{Al}_x)_2$ over a wide concentration range of Al from a nearly ferromagnetic to a weakly ferromagnetic phase. The values of $1/T_1 T$ from low temperature to high temperature were found to be well described by the self-consistent renormalization theory of spin fluctuations. From the analysis of $1/T_1 T$ the characteristic energy width of the dynamical spin-fluctuation spectrum is systematically estimated through this concentration range. It was found that these widths have quite different values on both sides of the critical concentration $x=0.12$, suggesting a discontinuous electronic-state change with the onset of weak itinerant ferromagnetism.

I. INTRODUCTION

The C15 cubic Laves-phases intermetallic compounds $Y(\text{Co}_{1-x}\text{Al}_x)_2$ in the concentration range $0.13 \leq x \leq 0.19$ show a typical weak itinerant-electron ferromagnetism.¹ For instance, the Curie temperature T_c and the spontaneous magnetic moment p_s have substantially small values, both of which have maximum values ($T_c=26$ K and $p_s=0.136\mu_B/\text{Co atom}$) for $x=0.15$. Although the magnetic susceptibility χ obeys the Curie-Weiss (CW) law at high temperatures above T_c , the effective paramagnetic moment p_{eff} deduced from the Curie constant C by assuming $C=N_A g^2 \mu_B^2 p_{\text{eff}}^2 / 3k_B$ [where N_A is Avogadro's number and g is the g factor (2 in this system)] has a much larger value [$(2-3)\mu_B$] than does p_s . The Arrott plots of magnetizations ($[M(T,H)]^2$ versus $H/M(T,H)$ plot) show good linearity with almost the same slope over a wide temperature region, typical for most weak itinerant ferromagnets. We further note that $[M(T,0)]^2$ and $[\chi(T)]^{-1}$ obey the $T^{4/3}$ relation over a fairly wide temperature range around T_c in good agreement with the prediction of the self-consistent renormalization (SCR) theory of spin fluctuations.²

Recently, developments of the quantitative SCR theory^{3,4} have enabled us to make comparisons between experiments and the theory. Because the nature of the spin fluctuations is characterized only by a few parameters, we can estimate them from the results of experiments such as magnetization measurement, neutron scattering, and NMR relaxation measurement. Using these parameters we can calculate other magnetic quantities such as T_c and χ in the framework of the SCR theory and compare them with experiments. In the $Y(\text{Co}_{1-x}\text{Al}_x)_2$ system in the weakly ferromagnetic phase, we can fairly well reproduce the observed temperature dependence of χ by using the spin-fluctuation parameters evaluated from the results of magnetic and NMR mea-

surements.⁵ The quantitatively good agreement between the experiments and the SCR theory has been now established in this $Y(\text{Co}_{1-x}\text{Al}_x)_2$ system⁵ even compared to other typical weak ferromagnets such as MnSi, Ni₃Al, Sc₃In, and ZrZn₂.³ Very recently, Takahashi⁶ has discussed the magnetic properties of weak itinerant ferromagnets based on the assumption that the mean-square local spin-fluctuation amplitude $\langle S_L^2 \rangle$, including the zero-point spin-fluctuation component, is almost conserved. He derived a relation among the spin-fluctuation parameters, leading to the reduction of the number of independent parameters by one compared with the SCR theory. He derived not only the same results of the SCR theory but a universal relation between the ratios of p_{eff}/p_s and T_c/T_0 . Here, T_0 is a parameter which was introduced to characterize the energy width of spin-fluctuation spectrum as will be defined later. This relation, which will be expressed as Eq. (19),⁶ gives a general interpretation of the Rhodes-Wohlfarth plot.⁷ In our previous paper,⁵ we showed the good agreement between the experiments and his theory as far as this $Y(\text{Co}_{1-x}\text{Al}_x)_2$ system is concerned.

In the present paper, we report the results of the magnetic and NMR measurements crossing through the transition from exchange-enhanced paramagnetic to weakly ferromagnetic concentration region of the $Y(\text{Co}_{1-x}\text{Al}_x)_2$ system. Measurements of the nuclear spin-lattice relaxation rate $1/T_1$ in this case also give us the quite important information in elucidating the nature of the dynamical spin-fluctuation spectrum. For all the exchange-enhanced paramagnets such as YCo₂, LuCo₂, TiBe₂, and Pd, both the linear electronic specific heat coefficient γ and the value of the susceptibility χ_0 at $T=0$ K are strongly enhanced by the mutual exchange interaction among electrons. Magnetic susceptibility sometimes shows a broad maximum at some temperature T_M .⁸⁻¹¹ Furthermore, it seems that the energy width of the spin-

fluctuation spectrum is correlated with the temperature T_M at which the χ - T curve shows a maximum or the Stoner enhancement factor $1/(1-\alpha_0)$, in the nearly ferromagnetic regime.⁸ The purpose of the present paper is to extend our detailed analysis of the previous study on this compound⁵ to the exchange-enhanced paramagnetic region and to assess the effectiveness of the SCR theory in this regime.

II. EXPERIMENTAL DETAILS

The samples were prepared from 99.99% pure Y and Co and 99.999% pure Al metals in an argon-arc furnace, followed by annealing at 950°C for two weeks in evacuated quartz tubes. No phase other than the C15 cubic Laves phase was detected by Debye-Scherrer x-ray analysis in Al concentrations at $x \leq 0.2$. The lattice constants almost obey Vegard's law.¹ The same sample was used in both magnetic and NMR measurements. For NMR measurements, the sample was crushed into fine powders in order to exclude the skin effect of rf field. The temperature variations of magnetic susceptibility $\chi(T)$ were measured by a torsion magnetic balance and a vibrating-sample magnetometer. The spin-echo NMR measurements were performed with a conventional phase-coherent-type spectrometer. The Knight shifts $K = (H_{\text{res}} - H_{\text{ref}})/H_{\text{res}}$ of ^{59}Co and ^{27}Al were determined by the resonance field H_{res} and the reference field $H_{\text{ref}} = \nu/\gamma_N$ with the resonance frequency ν and the known nuclear gyromagnetic ratios of $\gamma_B^{59\text{Co}} = 1.0054$ and $\gamma_N^{27\text{Al}} = 1.1094$ (in units of $2\pi 10^3 \text{ rad/sec Oe}$). The nuclear spin-lattice relaxation time T_1 was measured by recording the recovery of the spin-echo intensity after the application of saturating comb pulses.

III. RESULTS AND ANALYSES

A. Magnetic susceptibility

As shown in Figs. 1 and 2, the temperature variations of the magnetic susceptibility show the systematic change depending upon x through the transition from the exchange-enhanced paramagnetic YCo_2 to the weakly itinerant ferromagnetic region of $x \geq 0.13$. For YCo_2 , the χ - T curve agrees well with those previously reported.¹²⁻¹⁴ The temperature T_M at which the peak occurs shifts toward low temperatures and comes around 10 K for $x = 0.11$. The magnetic susceptibilities χ_0 and χ_M at $T = 0$ K and $T = T_M$ are strongly exchange enhanced due to the large Stoner enhancement factor $1/(1-\alpha_0)$. The observed values of the linear specific heat coefficient γ , for this system¹⁵ exhibit paramagnon-enhanced large values. For example, the observed value of γ for YCo_2 has been reported to come between 24 and 36 mJ/mol K^2 ,¹⁵⁻¹⁷ while the calculated value from the band theory was reported to be 13.7 mJ/mol K^2 ,¹⁸ the observed values of γ are enhanced about twice as large as the estimation from the calculated density of states. The observed values of T_M , χ_0 , χ_M , and γ are shown in Table I. We have estimated the Stoner enhancement factor $1/(1-\alpha_0)$ by comparing the observed uniform suscepti-

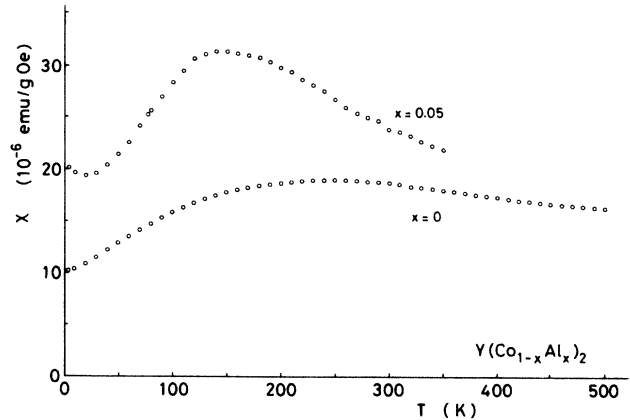


FIG. 1. Temperature variations of magnetic susceptibility χ of $\text{Y}(\text{Co}_{1-x}\text{Al}_x)_2$ with $x = 0.00$ and 0.05 .

bility with the density of states deduced from the observed γ (Ref. 15) by assuming that the enhancement of γ is two. The estimated values of $1/(1-\alpha_0)$ are also shown in Table I. As seen from this table the enhancement is substantially large and increases rapidly toward the appearance of ferromagnetism with increasing x . The generalized susceptibility for wave vector q in the interacting system $\chi(q)$ is also enhanced and given as

$$\chi(q) = \chi_0(q) / \{1 - \alpha_0[\chi_0(q)/\chi_0(0)]\} \quad (1)$$

with $\chi_0(q)$ and $\chi_0(0)$ being the dynamical susceptibility for noninteracting system and its uniform component. Here, the ratio of the enhancement of $\chi(q)$ to that of $\chi(0)$ is the important quantity to see the behavior of $\chi(q)$. The modification factor for electron-electron interaction $\mathcal{H}(\alpha_0)$ in the modified Korringa relation of the nuclear

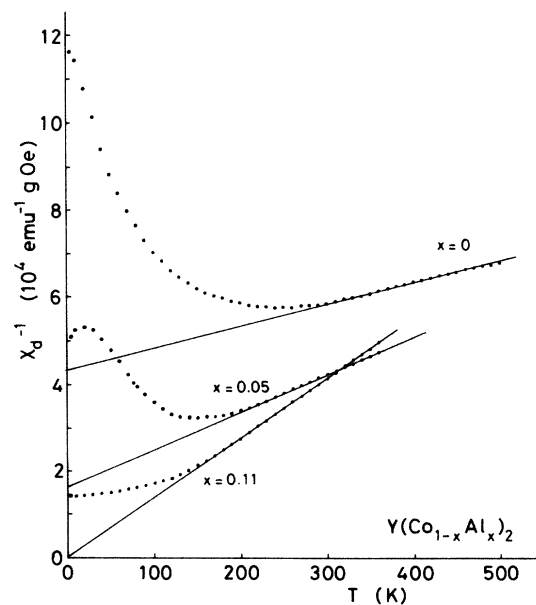


FIG. 2. Temperature variations of the inverse d -spin susceptibility $1/\chi_d$ of $\text{Y}(\text{Co}_{1-x}\text{Al}_x)_2$ with $x = 0.00, 0.05$, and 0.11 .

TABLE I. The temperature T_M at which χ shows maximum, the magnetic susceptibility χ_0 and χ_M at $T=0$ K and T_M , the linear electronic specific-heat coefficient γ , the Stoner enhancement factor $1/(1-\alpha_0)$, and the ratio $\mathcal{H}(\alpha_0)$ in the $Y(\text{Co}_{1-x}\text{Al}_x)_2$ system.

x	T_M (K)	χ_0 (10^{-3} emu/mol Oe)	χ_M (10^{-3} emu/mol Oe)	γ (mJ/mol K ²)	$1/(1-\alpha_0)$	$\mathcal{H}(\alpha_0)$
0.00	250	2.17	3.93	24-36	8-13	0.19-0.28
0.05	145	4.21	6.39	31	19	0.14
0.11	~ 10	13.9	14.0	45	44	0.04

spin-lattice relaxation time in the random-phase-approximation (RPA) theory includes this enhancement by the following expression:

$$\mathcal{H}(\alpha_0) = \left\langle \frac{(1-\alpha_0)^2}{\{1-\alpha_0[\chi_0(q)/\chi_0(0)]\}^2} \right\rangle_{\text{FS}}, \quad (2)$$

where $\langle \rangle_{\text{FS}}$ denotes the average over the wave vectors connecting two points on the Fermi surface. Moriya¹⁹ and Narath and Weaver²⁰ calculated the values of $\mathcal{H}(\alpha_0)$ based on the RPA theory using the electron-gas-like band and only taking account of the intra-atomic Coulomb interaction. They found $\mathcal{H}(\alpha_0)$ is close to 1 when $\chi(q)$ is almost uniformly enhanced in the q space as in the case of a local-moment system, while $\mathcal{H}(\alpha_0)$ is very small, of the order of $(1-\alpha_0)$, in the case of $\chi(q)$ enhanced only in a small- q region. In Table I we showed the value of $\mathcal{H}(\alpha_0)$ corresponding to the estimated value of α_0 . Through the whole concentration range studied here $\mathcal{H}(\alpha_0)$ is always much smaller than 1 as shown in Table I, implying that $\chi(q)$ is enhanced only in a limited small region around $q \sim 0$. We note here that the value of $\mathcal{H}(\alpha_0)$ estimated in this way can be compared fairly well with the directly measured one from the $1/T_1$ experiment as will be discussed in the later section.

The d -spin susceptibility χ_d has been estimated from the K versus χ plot as will be described in the next section. We found that $1/\chi_d$ shows the CW law at high temperatures as shown in Fig. 2. From the value of the Curie constant C we have estimated the value of p_{eff} in the paramagnetic region. We show the value of p_{eff} in Fig. 3 together with p_s observed in the ferromagnetic re-

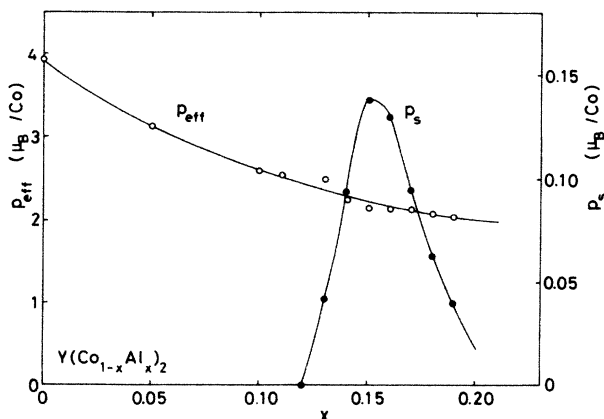


FIG. 3. Effective paramagnetic moment p_{eff} and spontaneous magnetic moment p_s plotted against Al concentration x in $Y(\text{Co}_{1-x}\text{Al}_x)_2$.

gion $0.13 \leq x \leq 0.19$. p_{eff} shows the gentle change from $2.5\mu_B/\text{Co}$ atom to $4.0\mu_B/\text{Co}$ atom as a function of x and its magnitude is fairly large compared with p_s .

B. Knight shift and hyperfine coupling constant

The typical spin-echo spectra of $Y(\text{Co}_{1-x}\text{Al}_x)_2$ for $x=0.05$ and 0.11 observed at the resonance frequency of 15.5005 MHz are shown in Fig. 4. These spectra resemble those in the paramagnetic state of the weakly itinerant ferromagnetic samples.⁵ The ^{59}Co spectrum has a simple shape for $x=0.05$ and 0.11 similar to $Y\text{Co}_2$ (Refs. 14 and 21) and shows a broadening due to the magnetic interactions depending upon temperature. The ^{27}Al spectrum shows the powder pattern with the quadrupole

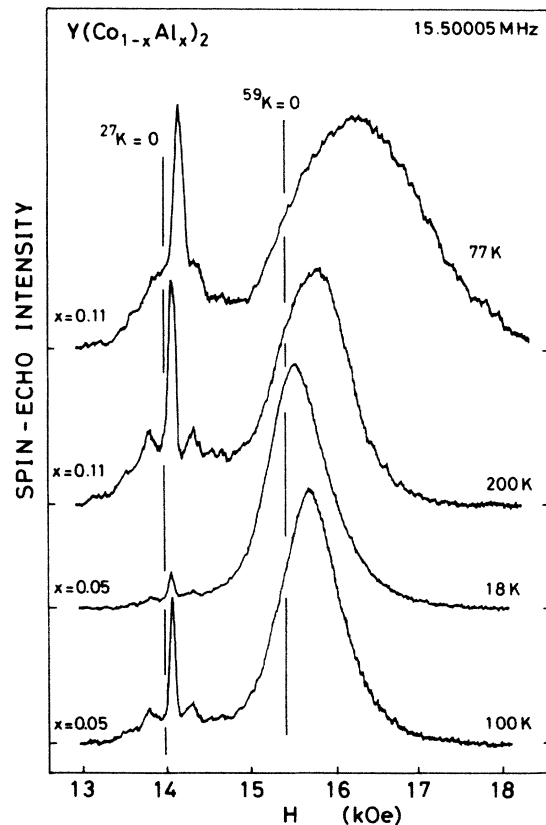


FIG. 4. Typical spin-echo NMR spectra of $Y(\text{Co}_{1-x}\text{Al}_x)_2$ with $x=0.05$ and 0.11 as functions of external field measured at a resonance frequency at 15.5005 MHz. The magnetic fields corresponding to zero Knight shift for both ^{59}Co and ^{27}Al , $^{59}K=0$ and $^{27}K=0$, are also shown.

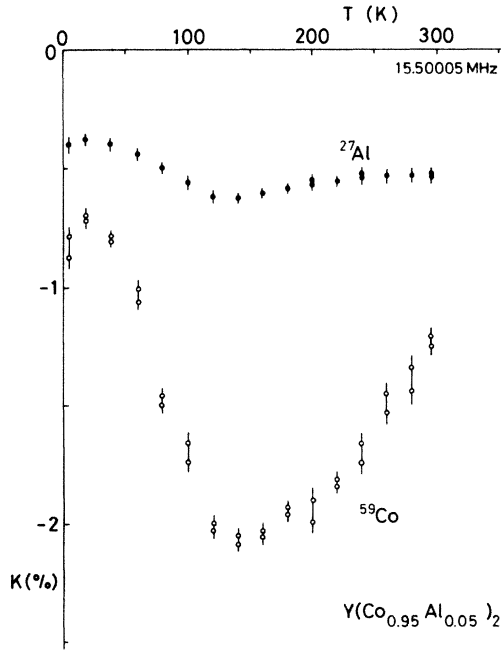


FIG. 5. Temperature dependence of the Knight shift K for ^{59}Co and ^{27}Al in $\text{Y}(\text{Co}_{0.95}\text{Al}_{0.05})_2$ at a resonance frequency of 15.50005 MHz.

splitting with the coupling constant $\nu_Q = [e^2qQ]/[h2I(2I-1)]$ of about 0.6 MHz. The resonance fields H_{res} for ^{59}Co and ^{27}Al have been found to show considerable temperature dependence. A typical example, the temperature dependence of the Knight shift K for ^{59}Co and ^{27}Al in the $\text{Y}(\text{Co}_{0.95}\text{Al}_{0.05})_2$ is shown in Fig. 5. In Fig. 6 the values of K are plotted as functions of χ with the temperature as an implicit parameter in the range between 4.2 K and room temperature. The K versus χ plots lie on a straight line for both ^{59}Co and ^{27}Al NMR. The result is almost the same for $x = 0.11$.

The measured susceptibility χ is decomposed as

$$\chi(T) = \chi_d(T) + \chi_{\text{orb}} + \frac{2}{3}\chi_{\text{CE}} + \chi_{\text{dia}}, \quad (3)$$

where $\chi_d(T)$ and χ_{orb} are the spin and orbital susceptibilities of d electrons, χ_{CE} is the spin susceptibility of conduction electrons, and χ_{dia} the diamagnetic susceptibility of core electrons. Only χ_d is assumed to be temperature dependent. Similarly, the Knight shift is expressed as

$$K(T) = K_d(T) + K_{\text{orb}} + K_{\text{CE}}, \quad (4)$$

with

TABLE II. Hyperfine coupling constant due to the d -electron spins; $A_{\text{hf}}(d)$ the coefficient $\mathcal{H}_0 = (1/T_1 T)_d / \chi_d$ and the Korringa relation term in $1/T_1 T$; β the d -spin contribution to $1/T_1 T$ at $T = 0$ K; $(1/T_1 T)_d^0$ and the ratio $\mathcal{H}(\alpha)$ in the $\text{Y}(\text{Co}_{1-x}\text{Al}_x)_2$ system.

x	Nucleus	$A_{\text{hf}}(d)$ (10^5 Oe/spin)	\mathcal{H}_0 ($\text{sec}^{-1} \text{K}^{-1} \text{emu}^{-1} \text{mol}$)	β ($\text{sec}^{-1} \text{K}^{-1}$)	$(1/T_1 T)_d^0$ ($\text{sec}^{-1} \text{K}^{-1}$)	$\mathcal{H}(\alpha)$
0.00	^{59}Co	-1.798	4300	2.5	7.5	0.29-0.31
0.05	^{59}Co	-1.199	2690	2.1	10.4	0.18
0.11	^{59}Co	-1.062	700.9	9.5	10.5	0.018
0.11	^{27}Al	-0.1543	10.29	0.038	0.137	0.010

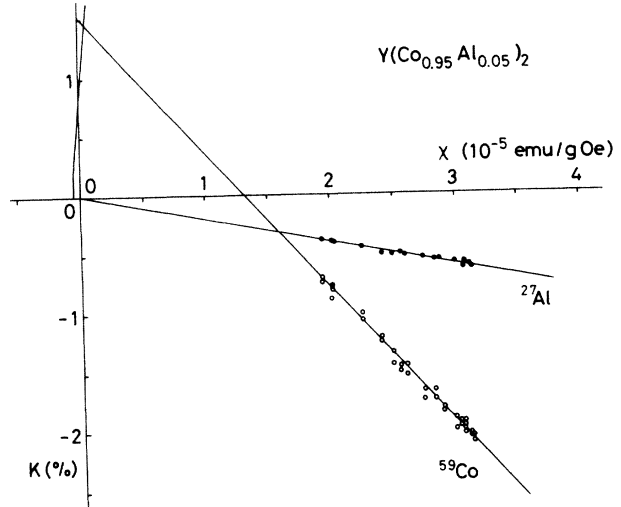


FIG. 6. K vs χ plot for ^{59}Co and ^{27}Al in $\text{Y}(\text{Co}_{0.95}\text{Al}_{0.05})_2$ with the temperature as an implicit parameter in the range between 4.2 and 300 K.

$$K_j = A_{\text{hf}}(j)\chi_j / [2(1-x)N_A g \mu_B],$$

$$j = d, \text{orb}, \text{ and CE},$$

$$g = \begin{cases} 2 & \text{for } j = d \text{ and CE}, \\ 1 & \text{for } j = \text{orb}, \end{cases} \quad (5)$$

where χ_j is expressed in the unit of emu/mol. $A_{\text{hf}}(j)$ is the hyperfine coupling constant which represents the hyperfine field per unit (spin or orbital) angular momentum on the respective Co or Al atom. In order to analyze the K versus χ plot of this system, we used the following values: $A_{\text{hf}}(\text{CE}) = 2.7 \times 10^6$ Oe obtained from the Hartree-Fock approximation by Watson and Freeman,²² $\chi_{\text{CE}} = 1.7 \times 10^{-9} \mu_B$ estimated by Cyrot and Lavagna (Ref. 23) $^{\text{Co}}\chi_{\text{dia}}$, $^{\text{Y}}\chi_{\text{dia}}$, and $^{\text{Al}}\chi_{\text{dia}}$ are estimated to be -5.51 , -10.19 , and -4.74 ($10^{-9} \mu_B/\text{atom}$), respectively, from relativistic Hartree-Fock approximations by Mendelsohn, Biggs, and Mann²⁴ and $A_{\text{hf}}(\text{orb}) = 5.7 \times 10^5$ Oe/ μ_B estimated from the Hartree-Fock calculation of $2\langle r^{-3} \rangle_{\text{av}} = 8.15 \times 10^{25} \text{ cm}^{-3}$ for Co^{2+} (Ref. 25) with a reduction factor of 0.75 in metallic system.²⁶ K_{CE} is estimated as 0.23% as a product of $H_{\text{hf}}(\text{CE})$ and χ_{CE} . From the values of χ_{dia} , χ_{CE} , K_{CE} , and $A_{\text{hf}}(\text{orb})$, the values of K_{orb} and χ_{orb} of Co are estimated as 1.4-2.4% and 2.3-4.2 ($10^{-8} \mu_B/\text{Co atom}$), respectively, for $x = 0, 0.05$, and 0.11. We can estimate the values of $A_{\text{hf}}(d)$ for ^{59}Co and ^{27}Al from the slope of K versus χ plots as shown in Table II and Fig. 7. $A_{\text{hf}}(d)$ for ^{59}Co shows substantial-

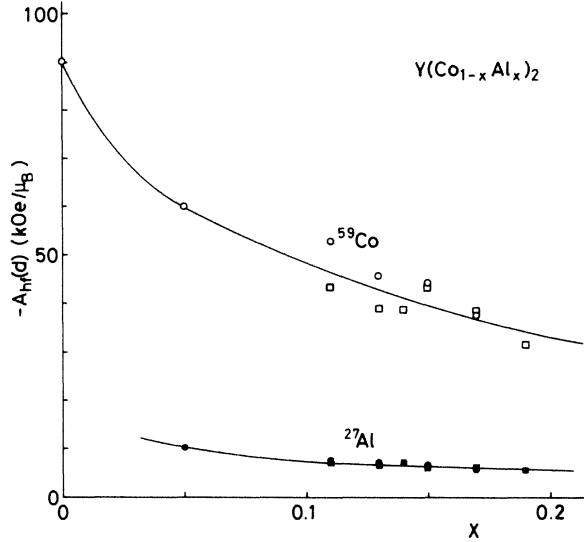


FIG. 7. Concentration dependence of the hyperfine coupling constant due to the d -electron spins. The circles represent $A_{\text{hf}}(d)$ estimated from the NMR results in the paramagnetic state and the square symbols from the NMR results in the ferromagnetic state.

ly large dependence on the Al concentration x as shown in Fig. 7, together with the values of A_{hf} for ^{59}Co and ^{27}Al in the ordered states of the ferromagnetic region $x \geq 0.13$.^{5,27} The absolute value of $A_{\text{hf}}(d)$ decreased remarkably with increasing x , suggesting that the positive contribution to the hyperfine field becomes important for large x . From this fact we expect the possibility of the appreciably large amount of $4s$ electron polarization through the s - d hybridization of the s - d exchange interaction at the Co sites.

C. Nuclear spin-lattice relaxation rate $1/T_1$

The temperature variations of the nuclear spin-lattice relaxation rate $1/T_1$ of ^{59}Co for $x = 0$ and 0.05 are shown in Fig. 8 in the form of $1/T_1 T$ versus T plot. Figure 9 shows that of $1/T_1 T$ of ^{59}Co and ^{27}Al for $x = 0.11$.

Generally, $1/T_1 T$ is decomposed as follows:

$$1/T_1 T = (1/T_1 T)_d + (1/T_1 T)_{\text{orb}} + (1/T_1 T)_s + (1/T_1 T)_{\text{dip}}, \quad (6)$$

where $(1/T_1 T)_d$ represents the contribution of d electron spins, $(1/T_1 T)_{\text{orb}}$ orbital moment contributions from p and d electrons, $(1/T_1 T)_s$ the Fermi contact contributions of s -conduction electrons, and $(1/T_1 T)_{\text{dip}}$ the contribution from the spin-dipolar interaction with p and d electrons. Here, we assume again that only $(1/T_1 T)_d$ depends on temperature while other terms are assumed to obey the Korringa relation $1/T_1 T = \text{constant}$. Although $(1/T_1 T)_{\text{dip}}$ due to d electrons is expected to show the similar temperature dependence as $(1/T_1 T)_d$, we neglected this term in comparison with $(1/T_1 T)_d$. As will be mentioned in Sec. IV, according to the SCR theory,²⁸ we

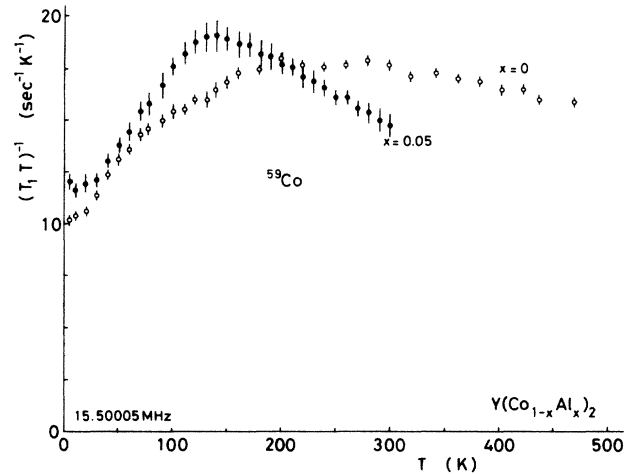


FIG. 8. Temperature dependence of the nuclear spin-lattice relaxation rate $1/T_1 T$ of ^{59}Co in $Y(\text{Co}_{1-x}\text{Al}_x)_2$ with $x = 0.00$ and 0.05 measured at a fixed frequency of 15.50005 MHz.

expect a linear relation between $(1/T_1 T)_d$ and χ_d :

$$1/T_1 T = \mathcal{K}_0 \chi_d + \beta, \quad (7)$$

where the first term represents $(1/T_1 T)_d$ and the second term β the sum of other contribution in Eq. (6). In Figs. 10 and 11 the values of $1/T_1 T$ are plotted against χ with the temperature as an implicit parameter. Furthermore, in Fig. 12 $(1/T_1 T)_d / \chi_d$ of ^{59}Co is plotted against temperature for $x = 0.00, 0.05$, and 0.11 . Actually, $1/T_1 T$ of ^{59}Co and ^{27}Al at finite temperatures satisfies Eq. (7). The values of the constants \mathcal{K}_0 and β are shown in Table II.

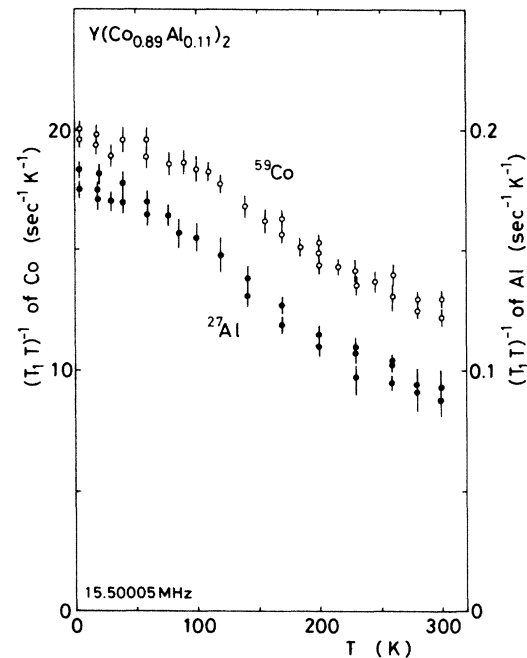


FIG. 9. Temperature dependence of the nuclear spin-lattice relaxation rate $1/T_1 T$ of ^{59}Co in $Y(\text{Co}_{0.89}\text{Al}_{0.11})_2$ measured at a fixed frequency of 15.50005 MHz.

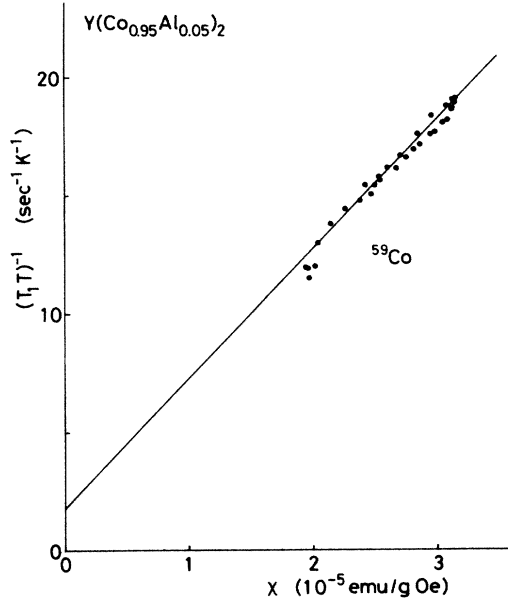


FIG. 10. $1/T_1T$ of ^{59}Co in $\text{Y}(\text{Co}_{0.95}\text{Al}_{0.05})_2$ plotted against the susceptibility χ with the temperature as an implicit parameter.

The coefficient \mathcal{H}_0 clearly shows the large dependence on Al concentration as shown in Fig. 13.

We next analyze the low-temperature data in terms of the RPA theory, hoping that the renormalization effect from thermal spin fluctuations may not be important at low temperatures. We have evaluated the value of $(1/T_1T)_d$ at $T=0$ K from Eq. (7) by using the above estimated values of \mathcal{H}_0 and β . The results are shown in

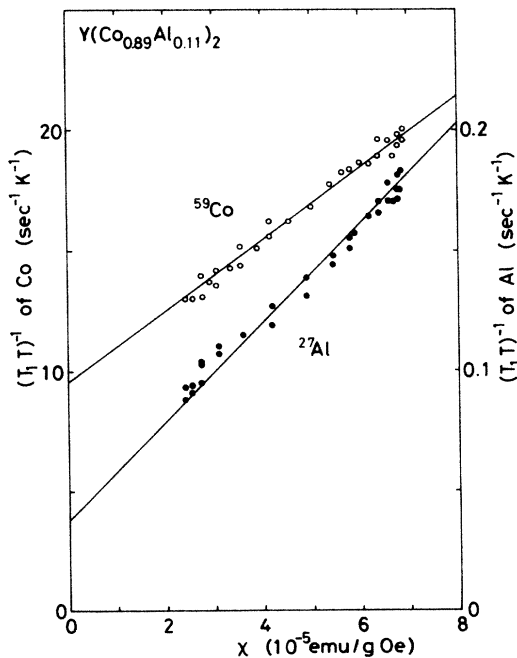


FIG. 11. $1/T_1T$ of ^{59}Co and ^{27}Al in $\text{Y}(\text{Co}_{0.89}\text{Al}_{0.11})_2$ plotted against the susceptibility χ with the temperature as an implicit parameter.

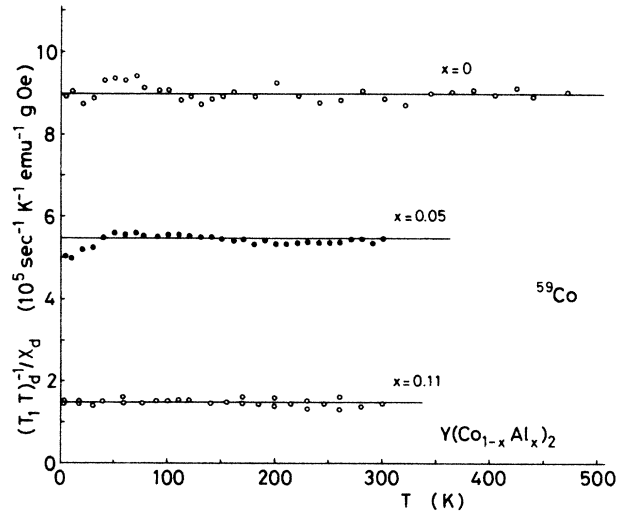


FIG. 12. Temperature dependence of $(1/T_1T)_d/\chi_d$ of ^{59}Co in $\text{Y}(\text{Co}_{1-x}\text{Al}_x)_2$ for $x=0.00, 0.05$, and 0.11 . $(1/T_1T)_d$ is almost proportional to χ_d , in good agreement with the SCR theory for weakly or nearly itinerant ferromagnets.

Table II as $(1/T_1T)_d^0$. In the RPA theory,^{29,30} $(1/T_1T)_d$ is written as

$$(1/T_1T)_d = K_d^2 (\pi \hbar k_B) (\gamma_N / \mu_B)^2 \times \left[\frac{1}{3} f^2 + \frac{1}{2} (1-f)^2 \right] \mathcal{H}(\alpha), \quad (8)$$

where f is the ratio of the density of $d\epsilon$ states to the total density of states at the Fermi level and the ratio $\mathcal{H}(\alpha)$ is determined by Eq. (2). Since the energy of $d\gamma$ state is higher than that of the $d\epsilon$ state due to the crystal field in the $C15$ structure, the $d\epsilon$ state is considered to be almost filled with d electrons of Co. Therefore, we can put f almost zero. If we use the observed values of $(1/T_1T)_d^0$, we

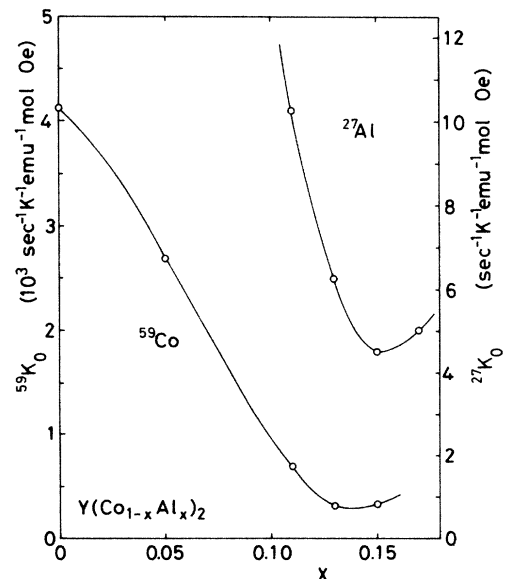


FIG. 13. Concentration dependence of \mathcal{H}_0 for ^{59}Co and ^{27}Al in $\text{Y}(\text{Co}_{1-x}\text{Al}_x)_2$, respectively.

can estimate values of $\mathcal{H}(\alpha)$ from Eq. (8) as shown in Table II. $\mathcal{H}(\alpha)$ shows good agreement with those values shown in Table I evaluated from the value of α according to Narath and Weaver.²⁰

Consequently, our analyses on $1/T_1T$ from a low-temperature to high-temperature region strongly suggest that $\chi(q)$ is enhanced only in a small- q region in our $Y(\text{Co}_{1-x}\text{Al}_x)_2$ system. This situation is characteristic to all the nearly or weakly itinerant ferromagnets. In such a case the mean-square local spin-fluctuation amplitude $\langle S_L^2 \rangle$ is not easily saturated with increasing temperature. Therefore, it is natural to assume the CW law of χ in this system is not caused by the conventional mechanism of the localized moment system but by the linear increase of the thermal part of $\langle S_L^2 \rangle$ with temperature as postulated by the SCR theory.²

IV. DISCUSSION

In order to treat the nearly or weakly ferromagnetic metals, the SCR theory³ assumes the following Lorentzian spectrum of the dynamical spin susceptibility $\chi(q, \omega)$ in a small- q, ω region,

$$\text{Im}\chi(q, \omega) = \frac{\chi(0, 0)}{1 + q^2/\kappa^2} \frac{\omega \Gamma_q}{\omega^2 + \Gamma_q^2}, \quad (9)$$

with Γ_q given by

$$\Gamma_q = \Gamma_0 q (\kappa^2 + q^2), \quad (10)$$

where the constant Γ_0 characterizes the energy width of the dynamical spin-fluctuation spectrum, whereas the parameter κ is the inverse of the correlation length. We introduce a parameter \bar{A} by

$$\kappa^2 = (1/2\bar{A})(N_0/\chi), \quad (11)$$

where N_0 is the number of atoms in the crystal. The value of \bar{A} gives the measure of dispersion of the wave-vector-dependent static susceptibility in the small- q region.³ This behavior of $\text{Im}\chi(q, \omega)$ has been confirmed from direct measurement by neutron scattering experiments for the typical weak itinerant ferromagnets MnSi (Refs. 31 and 32) and Ni_3Al .^{33,34} For parameters Γ_0 and \bar{A} we introduce two temperature scales T_0 and T_A as follows:

$$T_0 = \Gamma_0 q_B^3 / 2\pi, \quad (12)$$

$$T_A = \bar{A} q_B^2, \quad (13)$$

where q_B is the effective zone boundary vector given by $(6\pi^2/v_0)^{1/3}$, v_0 the volume per magnetic atom. In the SCR theory, nature of the spin fluctuations is characterized by a set of relatively small number of parameters $\alpha, p_s, \bar{F}_1, T_A$, and T_0 (\bar{F}_1 is the coefficient of the M^4 term in the Landau expansion of free energy which will be determined from the slope of Arrott plots). For theoretical details, see the Appendix. The SCR theory predicts some relations among these parameters. For instance, T_C is given as,

$$T_C^{4/3} = \frac{p_s^2 T_A T_0^{1/3}}{60c\alpha}, \quad (14)$$

with

$$c = 3^{-3/2} (1/2\pi)^{1/3} \Gamma(4/3) \zeta(4/3) = 0.3353. \dots \quad (15)$$

If we know enough number of parameters from experiments, we can check these relations and the quantitative validity of the SCR theory, as has been done successfully for several weak itinerant ferromagnets.³⁻⁵

The parameter Γ_0 can be deduced from the measurement of the nuclear spin relaxation rate $(1/T_1T)_d$. In terms of the imaginary part of the dynamical susceptibility for d electrons, $(1/T_1T)_d$ is generally expressed as follows:

$$(1/T_1T)_d = 2\gamma_N^2 k_B \sum_q A_{\text{hf}}(q)^2 \text{Im}\chi(q, \omega_0) / \omega_0, \quad (16)$$

where $A_{\text{hf}}(q)$ is the wave-number-dependent hyperfine coupling constant and ω_0 the NMR frequency. Since for weak itinerant ferromagnets contributions from small- q components dominate in the above q summation, $A_{\text{hf}}(q)$ is well approximated by $A_{\text{hf}}(0)$. By putting Eqs. (7) and (10) into Eq. (16), we obtain the d spin contribution to $1/T_1T$ in Eq. (7) together with the relation between Γ_0 and \mathcal{H}_0 as³

$$(1/T_1T)_d = \mathcal{H}_0 \chi_d \quad (17)$$

with

$$\mathcal{H}_0 = \frac{[\gamma_N A_{\text{hf}}(d)]^2 v_0}{4\pi^2 \Gamma_0 \mu_B}. \quad (18)$$

From Eq. (18), we can estimate Γ_0 from the observed values of \mathcal{H}_0 , $A_{\text{hf}}(d)$, and v_0 , and then, T_0 from Eq. (12). The estimated values of Γ_0 and T_0 are shown in Table III together with the value of v_0 for $x = 0.00, 0.05$, and 0.11 . T_0 is also shown as a function of Al concentration in Fig. 14 together with T_C in the ferromagnetic region. The values of T_0 estimated from ^{59}Co and ^{27}Al NMR differ for high concentration x . Since $(1/T_1T)_d$ is proportional to $\gamma_N^2 A_{\text{hf}}(d)^2$, this discrepancy in T_0 is ascribed to the difference between the values of $(1/T_1T)_d / [\gamma_N A_{\text{hf}}(d)]^2$ for ^{59}Co and ^{27}Al . We suppose that only A_{hf} for ^{59}Co shows the large concentration dependence compared with that for ^{27}Al , which gives rise to the concentration-dependent discrepancy of T_0 . If we use the relation derived by Takahashi⁶ as

$$15\bar{F}_1 T_0 = 4k_B T_A^2, \quad (19)$$

T_0 can be also estimated from the following relation:

TABLE III. Estimated values of Γ_0 and T_0 together with v_0 (see text).

x	Nucleus	v_0 (\AA^3)	Γ_0 ($\text{\AA}^3 k_B$)	T_0 (K)
0.00	^{59}Co	23.50	909	365
0.05	^{59}Co	25.00	724	273
0.11	^{59}Co	27.17	2687	932
0.11	^{27}Al	27.17	4423	1534

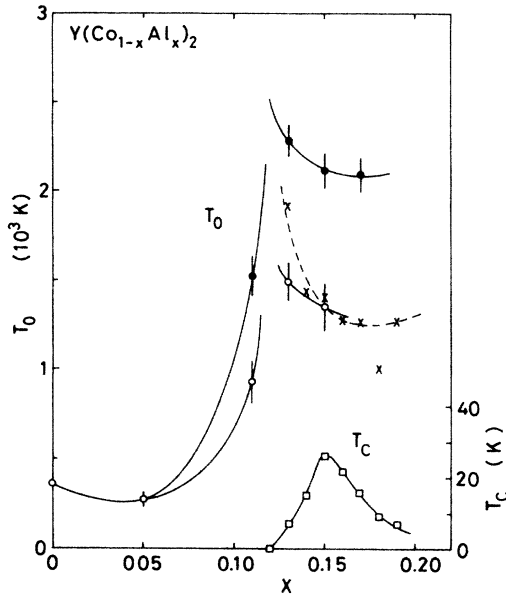


FIG. 14. Concentration dependence of T_0 in $Y(\text{Co}_{1-x}\text{Al}_x)_2$ together with that of T_C . Open circles represent T_0 evaluated from ^{59}Co NMR and closed circles those from ^{27}Al NMR. Crosses show T_0 estimated from the magnetization measurements by using Takahashi's theory.⁶

$$(T_0)^{5/6} = \frac{8c}{15p_s^2} \left(\frac{k_B}{\bar{F}_1} \right)^{1/2} T_C^{4/3}. \quad (20)$$

Here, only by using parameters from the magnetic measurements⁵ we can evaluate the values of T_0 for the ferromagnetic samples. The values of T_0 thus evaluated are also shown in Fig. 14 by cross symbols. We have a good agreement between the estimated values of T_0 directly from observed $(1/T_1 T)_d$ and the one from Eq. (20) as seen in Fig. 14. It should be noted that estimated values of T_0 are always substantially large compared with the value of T_C in this system, which is characteristic to the nearly or weakly itinerant ferromagnetic regime.³ The most interesting feature of the concentration dependence of T_0 is that T_0 has quite different values in both sides of the critical concentration $x \sim 0.12$ of the appearance of ferromagnetism. This suggests that the electronic state change does not occur continuously but discontinuously at this concentration. This picture seems to be consistent with the results of the high field magnetization measurements at 4.2 K, in which the distinct metamagnetic transition originated in YCo_2 is broadened and disappears on the onset of ferromagnetism.³⁵ This situation can be understood based on a simple model of free energy as a function of the uniform magnetization shown in Fig. 15(a) and 15(b). We assume that Fig. 15(a) is realized for the paramagnetic phase $x \leq 0.12$. When the high field is applied on the system (the situation under the critical field H_C of the metamagnetic transition is shown by the broken line), the magnetization rapidly increases from M_1 to M_2 as the first-order transition, and the electronic state of $3d$ electrons will also change dramatically. If the

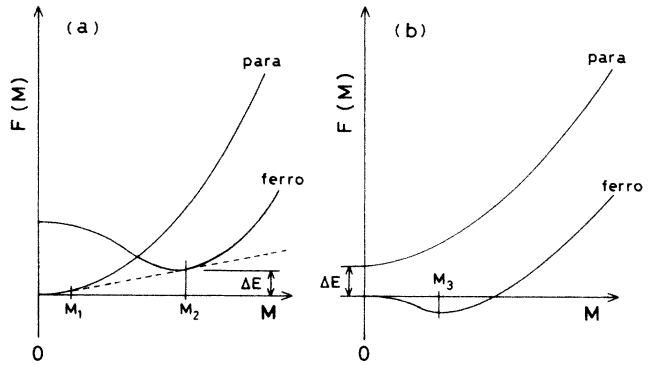


FIG. 15. Model of free energy $F(M)$ as a function of magnetization M . (a) and (b) Correspond to the cases of $x \leq 0.12$ and $x \geq 0.12$, respectively.

energy difference between these two states ΔE is very small, relative position of these energy levels is easily upset. Therefore, we assume for $x \geq 0.12$ the situation as shown in Fig. 15(b). The ground state becomes ferromagnetic in this case with the spontaneous magnetization of M_3 and the metamagnetic transition does not take place any more. The large change of hyperfine coupling constant for ^{59}Co may also be understood associated with the discontinuous change of the electronic state.

V. CONCLUSION

The magnetic properties of $Y(\text{Co}_{1-x}\text{Al}_x)_2$ have been investigated by the spin-echo NMR experiments from a microscopic and dynamical point of view. The observed temperature dependence of χ and $(1/T_1 T)_d$ has been well described by the SCR theory over the wide temperature range. From the analysis of the Knight shift and $1/T_1$ at low temperatures we conclude that the spin fluctuations in this system have a local character in the q space, consistent with the appearance of the nearly and weakly itinerant-electron ferromagnetism in this system. From the results of $(1/T_1 T)_d$ the characteristic spin-fluctuation temperature T_0 has been determined through the whole concentration region of $x \leq 0.19$ according to the framework of the SCR theory.³ T_0 has a substantially large value in contrast with the small value of T_C similarly to other typical weak itinerant systems.³ The concentration dependence of T_0 shows quite interesting drastic change around $x = 0.12$, suggesting that the electronic state of $3d$ electrons changes discontinuously around this concentration. This fact shows a good agreement with the results of recent high field magnetization measurements.³⁵

The remaining problem is how to understand the origin of the maximum in the $\chi - T$ curve for some strongly exchange-enhanced paramagnetic cases. One idea, due to Moriya,³⁶ is to associate this feature with the negative mode-mode coupling among spin-fluctuation modes, which comes from the negative curvature of the density of states at the Fermi level. The rapid increase of χ at low temperatures and the origin of maximum of χ in FeSi were explained by this mechanism.³⁷ Based on the same mechanism, Takagi and Yasuoka³⁸ explained the temper-

ature dependence of χ in TiBe_2 . On the other hand, based on the Stoner model Wohlfarth pointed out the importance of fine structures of the density-of-states curve near the Fermi level as the origin of the χ maximum.³⁹ The appearance of the maximum in χ seems to be quite generally not confined to the nearly itinerant ferromagnetic cases. Recently, a lot of heavy Fermion systems has often been found to exhibit similar behavior.⁴⁰ We notice here the existence of some correlations⁸ between T_0 and T_M or T_0 and $1/(1-\alpha)$ in the small-concentration region of this system. The value of T_0 decreases with decreasing T_M or with increasing $1/(1-\alpha)$; $T_0=365$ K, $T_M=250$ K, $1/(1-\alpha)=8-13$ for $x=0.0$; $T_0=273$ K, $T_M=145$ K, $1/(1-\alpha)=19$ for $x=0.05$. In order to understand the origin of the maximum in the χ - T curve associated with these correlations, further experimental studies and theoretical developments are needed.

ACKNOWLEDGMENTS

The authors would like to thank Professor T. Moriya for valuable discussions. One of the authors (K.Y.) is grateful to Professor Y. Nakamura for introducing him to itinerant magnetism.

APPENDIX: THEORETICAL ASPECTS AND EXPERIMENTS

This section is written for help in understanding theoretical concepts and the meaning of the spin-fluctuation parameters, and also as a guide for the present analysis. The theoretical study of this section is in accordance with Takahashi and Moriya³ and Moriya.⁴¹

In the Hartree-Fock Stoner theory, the free energy per magnetic atom is given by the Landau expansion as

$$F(M) = \frac{1-\alpha}{2\chi_0} M^2 + \frac{1}{4} \bar{F}_1 M^4 + \cdots - 2\mu_B H M \quad (\text{A1})$$

with

$$\alpha = I\rho = 2I\chi_0, \quad (\text{A2})$$

$$F_1 = \rho^3 \bar{F}_1 = (\rho'/\rho)^2 - (\rho''/3\rho), \quad (\text{A3})$$

where M is the magnetization in units of $2\mu_B$ per magnetic atom, χ_0 the susceptibility in units of $4\mu_B^2$ per magnetic atom without electron-electron interaction, ρ the density of state per magnetic atom at the Fermi level, ρ' and ρ'' its derivatives, and I the intra-atomic exchange integral.

The magnetic equation of states is determined by minimizing $F(M)$ with respect to M as

$$\bar{F}_1 M^2 = \frac{2\mu_B H}{M} + \frac{2(\alpha-1)}{\rho}. \quad (\text{A4})$$

This equation is exactly equivalent to the Arrott plot expression of magnetization. Therefore, we can obtain the M^4 term coefficient \bar{F}_1 from the slope of the Arrott plot. In particular the spontaneous magnetization in units of μ_B per magnetic atom at $T=0$ K is obtained by

$$\begin{aligned} p_s = 2M(0) &= 2 \left[\frac{2(\alpha-1)}{\bar{F}_1 \rho} \right]^{1/2} \\ &= 2\rho \left[\frac{2(\alpha-1)}{F_1} \right]^{1/2}. \end{aligned} \quad (\text{A5})$$

These Hartree-Fock expressions, however, are not correct at finite temperatures, since the effects of spin fluctuations are not included in the system. In the SCR theory, in order to renormalize the effects of spin fluctuations into the thermally equilibrium state self-consistently, the contribution of the couplings among different modes of spin fluctuations $\lambda(q, \omega)$ has been introduced into the RPA expression of the transverse dynamical susceptibility as

$$\chi^{-+}(q, \omega) = \frac{\chi_0^{-+}(q, \omega)}{1 + \lambda(q, \omega) - I\chi_0^{-+}(q, \omega)}. \quad (\text{A6})$$

For a weakly itinerant-electron ferromagnet, $\lambda(q, \omega)$ can be approximated by $\lambda(0, 0)$. A rotationally invariant formalism of the SCR theory^{42,43} derives the following expression of λ :

$$\lambda(q, \omega) \rightarrow \lambda \sim \frac{5}{4} \alpha^2 \rho^{-2} F_1 T \sum_m \sum_q \chi^{-+}(q, i\omega_m), \quad (\text{A7})$$

where $\omega_m = 2\pi mT$ and m is an integer. This relation can also be derived from phenomenological theories.^{44,45} In the SCR theory we need to solve Eqs. (A6) and (A7) to obtain λ and $\chi^{-+}(q, \omega)$. For that reason, the following expansion form of the noninteracting dynamical susceptibility for small q and small ω/q has been introduced for weak ferromagnetic metals as

$$\chi_0^{-+}(q, \omega) = \chi_0^{-+}(0, 0)(1 - Aq^2 + \cdots + iC\omega/q). \quad (\text{A8})$$

The expression of λ contains the contributions of zero-point and thermal spin fluctuations. Since the former is expected to be temperature independent in the weak ferromagnetic regime, we have deduced λ from these equations by leaving only the thermal contribution as

$$\begin{aligned} \lambda &= \frac{5\alpha}{2\pi\rho} (1 + \delta) F_1 \\ &\times \sum_q \int_0^\infty d\omega \frac{1}{\exp(\omega/T) - 1} \frac{C\omega/q}{(\delta + Aq^2)^2 + (C\omega/q)^2}, \end{aligned} \quad (\text{A9})$$

with

$$\delta = \chi_0/\alpha\chi = (1 - \alpha + \lambda)/\alpha. \quad (\text{A10})$$

For the dynamical susceptibility, we note the relation $\chi^{-+}(q, \omega) = 2\chi(q, \omega)$ and introduce the following parameters as:

$$\kappa^2 = \delta/A = \frac{\rho}{2\alpha\chi A} \equiv (1/2\bar{A})(N_0/\chi), \quad (\text{A11})$$

$$\Gamma_q = (A/C)q(\kappa^2 + q^2) \equiv \Gamma_0 q(\kappa^2 + q^2). \quad (\text{A12})$$

Therefore, we have $\chi(q, \omega)$ as Eq. (9). Here, \bar{A} and Γ_0 are very important parameters to characterize the form of

$\chi(q, \omega)$. The value of \bar{A} and Γ_0 are determined directly by the neutron scattering which measures

$$S(q, \omega) = 2[1 - \exp(-\omega/T)]^{-1} \text{Im}\chi(q, \omega). \quad (\text{A13})$$

As described in Sec. IV, this form of $\chi(q, \omega)$ in Eq. (9) was confirmed to be valid for weak ferromagnets by neutron scattering experiments.³¹⁻³⁴ The parameter Γ_0 , which means the energy width of the spin-fluctuation spectrum of Eq. (9), is also determined by the relation between the nuclear spin-lattice relaxation time and the static susceptibility as in Eqs. (17) and (18).

As a matter of convenience for treatments, the characteristic temperatures T_0 and T_A are introduced for Γ_0 and \bar{A} as Eqs. (12) and (13). As seen in Eqs. (9)-(13), (A9), and (A10), the spin fluctuations are expressed in terms of only following five parameters which can be

determined by the experiments:

$$\begin{aligned} \alpha, p_s (\text{or } \rho), \bar{F}_1, \bar{A} &= AN_0/\rho \quad (\text{or } T_A), \\ \Gamma_0 &= A/C \quad (\text{or } T_0). \end{aligned} \quad (\text{A14})$$

In the SCR theory, consequently, we can describe the magnetic quantities by using these five parameters. For example, T_C is expressed by Eqs. (14) and (15). The magnetic susceptibility above T_C is also written by these parameters in an integral form by using the digamma function. As mentioned in the text, we have obtained quantitative agreements between experiments and theoretical calculations by using spin-fluctuation parameters which have been evaluated by other experiments such as neutron scattering and NMR relaxation time measurements.³⁻⁵

*Present address: Group P-10, Los Alamos National Laboratory, Los Alamos, NM 87545.

¹K. Yoshimura and Y. Nakamura, *Solid State Commun.* **56**, 767 (1985).

²T. Moriya and A. Kawabata, *J. Phys. Soc. Jpn.* **34**, 639 (1973); **35**, 669 (1973).

³Y. Takahashi and T. Moriya, *J. Phys. Soc. Jpn.* **54**, 1592 (1985).

⁴G. G. Lonzarich and L. Taillefer, *J. Phys. C* **18**, 4339 (1985).

⁵K. Yoshimura, M. Takigawa, Y. Takahashi, H. Yasuoka, and Y. Nakamura, *J. Phys. Soc. Jpn.* **56**, 1138 (1987).

⁶Y. Takahashi, *J. Phys. Soc. Jpn.* **55**, 3553 (1986).

⁷P. R. Rhodes and E. P. Wohlfarth, *Proc. R. Soc. London* **273**, 247 (1963).

⁸K. Yoshimura, K. Fukamichi, H. Yasuoka, and M. Mekata, *J. Phys. Soc. Jpn.* **56**, 3652 (1987).

⁹K. Ishiyama, A. Shinogi, and K. Endo, *J. Phys. Soc. Jpn.* **53**, 2456 (1984).

¹⁰S. Takagi, H. Yasuoka, J. L. Smith, and C. Y. Huang, *J. Phys. Soc. Jpn.* **53**, 3210 (1984).

¹¹M. Takigawa and H. Yasuoka, *J. Phys. Soc. Jpn.* **51**, 787 (1982).

¹²R. Lemaire, *Cobalt* **33**, 201 (1966).

¹³E. Burzo, *Int. J. Magn.* **3**, 161 (1972).

¹⁴K. Yoshimura, T. Shimizu, M. Takigawa, H. Yasuoka, and T. Nakamura, *J. Phys. Soc. Jpn.* **53**, 503 (1984).

¹⁵E. Fukami, H. Wada, M. Shiga, and Y. Nakamura (unpublished).

¹⁶D. Bloch, D. L. Camphausen, J. Voiron, J. B. Ayasse, A. Berton, and J. Chaussey, *C. R. Acad. Sci. (Paris)* **275**, B-601 (1972).

¹⁷Y. Muraoka, M. Shiga, and Y. Nakamura, *J. Phys. Soc. Jpn.* **42**, 2067 (1977).

¹⁸H. Yamada, J. Inoue, K. Terao, S. Kanda, and M. Shimizu, *J. Phys. F* **14**, 1943 (1984).

¹⁹T. Moriya, *J. Phys. Soc. Jpn.* **18**, 516 (1963).

²⁰A. Narath and H. T. Weaver, *Phys. Rev.* **175**, 373 (1968).

²¹S. Hirose and Y. Nakamura, *J. Phys. Soc. Jpn.* **51**, 2464

(1982).

²²R. E. Watson and A. J. Freeman, *Phys. Rev.* **123**, 2027 (1961).

²³M. Cyrot and M. Lavagna, *J. Phys. (Paris)* **40**, 763 (1979).

²⁴L. B. Mendelsohn, F. Biggs, and J. B. Mann, *Phys. Rev. A* **2**, 1130 (1970).

²⁵G. Burns, *Phys. Rev.* **128**, 2121 (1962).

²⁶A. M. Clogston, V. Jaccarino, and Y. Yafet, *Phys. Rev.* **134**, A650 (1964).

²⁷K. Yoshimura and Y. Nakamura (unpublished).

²⁸T. Moriya and K. Ueda, *Solid State Commun.* **15**, 169 (1974).

²⁹Y. Yafet and V. Jaccarino, *Phys. Rev.* **133**, A1630 (1964).

³⁰T. Moriya, *J. Phys. Soc. Jpn.* **19**, 681 (1964).

³¹Y. Ishikawa, Y. Noda, C. Fincher, and G. Shirane, *Phys. Rev. B* **25**, 254 (1982).

³²Y. Ishikawa, Y. Noda, Y. J. Uemura, C. F. Majkrzak, and G. Shirane, *Phys. Rev. B* **31**, 5884 (1985).

³³N. R. Bernhoeft, I. Cole, G. G. Lonzarich, and G. L. Squires, *J. Appl. Phys.* **53**, 8204 (1982).

³⁴N. R. Bernhoeft, G. G. Lonzarich, P. W. Mitchell, and D. Mck. Paul, *Phys. Rev. B* **28**, 422 (1983).

³⁵T. Sakakibara, T. Goto, K. Yoshimura, M. Shiga, and Y. Nakamura, *Phys. Lett. A* **117**, 243 (1986).

³⁶T. Moriya, *J. Magn. Magn. Mater.* **14**, 1 (1979).

³⁷Y. Takahashi and T. Moriya, *J. Phys. Soc. Jpn.* **54**, 2287 (1985).

³⁸S. Takagi and H. Yasuoka, *J. Phys. Soc. Jpn.* **54**, 2287 (1985).

³⁹E. P. Wohlfarth, *J. Phys. Lett.* **41**, L-563 (1980).

⁴⁰For example, J. J. M. Franse, A. de Visser, A. Menovsky, and P. H. Frigs, *J. Magn. Magn. Mater.* **52**, 61 (1985).

⁴¹T. Moriya, *Spin Fluctuations in Itinerant Electron Magnetism* (Springer, Berlin, 1985); *A Unified Picture of Magnetism*, edited by H. Capellmann (Springer, Berlin, 1987).

⁴²A. Kawabata, *J. Phys. F* **4**, 1477 (1974).

⁴³T. Moriya, *J. Phys. Soc. Jpn.* **40**, 933 (1976).

⁴⁴G. G. Lonzarich, *J. Magn. Magn. Mater.* **45**, 43 (1984).

⁴⁵T. Moriya and K. Usami, *Solid State Commun.* **34**, 95 (1980).